In vivo three-photon imaging of deep cerebellum

Mengran Wang, Tianyu Wang, Chunyan Wu, Bo Li, Dimitre G. Ouzounov, et al.

Mengran Wang, Tianyu Wang, Chunyan Wu, Bo Li, Dimitre G. Ouzounov, David Sinefeld, Akash Guru, Hyung-Song Nam, Mario R. Capecchi, Melissa R. Warden, Chris Xu, "In vivo three-photon imaging of deep cerebellum," Proc. SPIE 10498, Multiphoton Microscopy in the Biomedical Sciences XVIII, 1049816 (23 February 2018); doi: 10.1117/12.2285406

SPIE.

Event: SPIE BiOS, 2018, San Francisco, California, United States

In vivo three-photon imaging of deep cerebellum

Mengran Wang*[a], Tianyu Wang [a], Chunyan Wu [a], Bo Li [a], Dimitre G. Ouzounov [a], David Sinefeld [a], Akash Guru[b], Hyung-Song Nam[c], Mario R. Capecchi[c], Melissa R. Warden[b], and Chris Xu[a]
[a]School of Applied and Engineering Physics, Cornell University, Ithaca, NY 14853
[b]Department of Neurobiology and Behavior, Cornell University, Ithaca, NY 14853
[c]Department of Human Genetics, University of Utah, Salt Lake City, UT 84112

ABSTRACT

We demonstrate three-photon microscopy (3PM) of mouse cerebellum at 1 mm depth by imaging both blood vessels and neurons. We compared 3PM and 2PM in the mouse cerebellum for imaging green (using excitation sources at 1300 nm and 920 nm, respectively) and red fluorescence (using excitation sources at 1680 nm and 1064 nm, respectively). 3PM enabled deeper imaging than 2PM because the use of longer excitation wavelength reduces the scattering in biological tissue and the higher order nonlinear excitation provides better 3D localization [1, 2]. To illustrate these two advantages quantitatively, we measured the signal decay as well as the signal-to-background ratio (SBR) as a function of depth. We performed 2-photon imaging from the brain surface all the way down to the area where the SBR reaches ~ 1, while at the same depth, 3PM still has SBR above 30. The segmented decay curve shows that the mouse cerebellum has different effective attenuation lengths at different depths, indicating heterogeneous tissue property for this brain region. We compared the third harmonic generation (THG) signal, which is used to visualize myelinated fibers, with the decay curve. We found that the regions with shorter effective attenuation lengths correspond to the regions with more fibers. Our results indicate that the widespread, non-uniformly distributed myelinated fibers adds heterogeneity to mouse cerebellum, which poses additional challenges in deep imaging of this brain region.
Keywords: three-photon microscopy, mouse cerebellum, quantitative comparison

1. INTRODUCTION

Multiphoton microscopy (MPM) revolutionized the field of microscopy by applying nonlinear interaction between light and matter and improved SBR performance by orders of magnitude. Two-photon microscopy (2PM) has been widely used in the field of biology and neuroscience by combining with a variety of fluorescence indicators. Despite the improvement in deep imaging, the depth penetration of 2PM is still limited in a densely labeled tissue sample[1]. Three-photon microscopy (3PM) improves the SBR limit by another few orders of magnitude, thus providing the ability to penetrate deeper into biological tissue which is unreachable for 2PM, such as the mouse hippocampus *in vivo*[2,3]. In this study, we performed a series of comprehensive quantitative comparison of 2PM and 3PM imaging in the mouse cerebellum[4,5] *in vivo* of blood vessels as well as neurons.

2. METHODS

We compared 2PM and 3PM in three experiments. We imaged fluorescein (FITC)-labeled blood vessels in the mouse cerebellum using 920 nm excitation and 1300 nm excitation for 2PM and 3PM, respectively. The excitation source for 3PM is a non-collinear optical parametric amplifier (NOPA, Spectra Physics) pumped by a chirped-pulse amplification system (Spirit, Spectra-Physics). The excitation source for 2PM is a mode-locked Ti:sapphire laser (Tsunami, Spectra Physics) operating at 920 nm. For vasculature labeling, we used adult wild-type mice (C57BJ/6J, 8-12 weeks) injected retro-orbitally with fluorescein dextran conjugate (10kMW, 10 mg, Thermal Fisher). Then we imaged Texas Red-labeled blood vessels using 1064 nm excitation and 1680 nm excitation for 2PM and 3PM, respectively. The excitation source for 3PM is an optical parametric amplifier (OPA, Opera-F, Coherent) pumped by a Monaco amplifier (Coherent), operating at 1680 nm. The excitation source for 2PM is a fiber laser system (Fianium FemtoPower, NKT Photonics). For vasculature labeling, we used adult wild-type mice (C57BJ/6J, 8-12 weeks) injected retro-orbitally with Texas Red dextran conjugate (70kMW, 25 mg, Thermal Fisher). In a third experiment, we used adult transgenic mice with tdTomato labeling (Lrigl-creER/Rosa 26Ai14, 8-10 weeks) to demonstrate neuronal imaging in mouse cerebellum for 2PM and 3PM with the 1064 nm excitation and 1680 nm excitation, respectively.

Multiphoton Microscopy in the Biomedical Sciences XVIII, edited by Ammasi Periasamy, Peter T. C. So, Karsten König, Xiaoliang S. Xie, Proc. of SPIE Vol. 10498, 1049816

3. RESULTS

We first compare 3-photon and 2-photon imaging of fluorescein-labeled blood vessels in mouse cerebellum. Due to the absorption and scattering by the biological tissue, the excitation power at the focus is attenuated relative to the power at the brain surface. Effective attenuation length (l_e) is used to describe the effect caused by absorption and scattering. The power at the focus can be described by:

$$P(z) = P(0)e^{-\frac{z}{l_e}}$$

Where z is the imaging depth below the brain surface, P(0) is the power at the surface, P(z) is the power at the depth z.

For 2PM (3PM), signal is proportional to the square (cubic) of the excitation power. Based on these relationships, we can calculate the effective attenuation lengths by plotting the normalized signal with depth (Figure 1a). Calculated effective attenuation lengths are labeled close to their corresponding curves. Although the curves are segmented, 3PM has longer effective attenuation lengths at all regions of the cerebellem.

For the SBR measurements, a line was drawn across a small blood vessel and the intensity profile is plotted along the line, we took the peak value of the measurement as the sum of signal and background and took the average value from -20~-10 μm and 10~20 μm as the background value, SBR is calculated based on the signal and background value. Here, we measured the SBR on several blood vessels with similar size in 2PM and 3PM (Figure 1c) at each depth and take the average as the representative SBR value for each depth (Figure 1b), we found that around 650 μm, SBR in 2PM reaches 1 while SBR in 3PM is still above 30. It's also shown (Figure 1c) that at deeper sites, images in 2PM is blurry and small features are hard to distinguish from the background whereas the images in 3PM still have high contrast. This is due to the higher order nonlinearity of 3PM, where signal is more localized with less out-of-focus background excitation.
Comparison of the 3D reconstruction of images at all depths for 2PM and 3PM is shown in Figure 1d, the imaging depth for 2PM is around 680 μm and imaging depth for 3PM is around 1020 μm. In order to understand the segmented decay curve in Figure 1a, we compared the 3D reconstruction of the third harmonic generation (THG), which is used to visualize the myelinate fibers in the cerebellum, with the decay curve (Figure 1e). From this comparison, we can see that whenever the THG shows more fiber distribution, there is a faster decay of the signal. More notably, at 800~1000 μm, there is strong white matter signal in the THG figure, and correspondingly in the decay curve, this is the area with shortest effective attenuation length. This comparison confirms that the segmental signal decay in the cerebellum is mostly due to the heterogeneous fiber distribution.
We then compared the performance of 2PM and 3PM for red fluorophores by imaging Texas Red-labeled blood vessels excited by 1064 nm and 1680 nm, respectively (Figure 2). It shows similar results as FITC. Here for 2PM, the background begins to take over the signal at a depth of 630 μm, whereas for 3PM, the SBR is still high down to 1120 μm. At around 510 μm, SBR in 2PM almost reaches 1 where SBR in 3PM is above 70. We note that these numbers cannot be compared to that in Figure 1 because of the different imaging locations and the highly heterogeneous nature of the cerebellum. Finally, we imaged tdTomato-labeled neurons in transgenic mice excited by 1064 nm and 1680 nm for 2PM and 3PM, respectively. For the SBR measurements here, we took the peak value of the measurement as the sum of signal and background and took the average value from -35~-20 μm only rather than both sides as the background value because the orientation of axons and dendrites are aligned on one side of the cell body, SBR is calculated based on the signal and background value (Figure 3c). We plotted the SBR value at each depth and found that around 770 μm, SBR in 2PM reaches 1 while SBR in 3PM is still above 20.

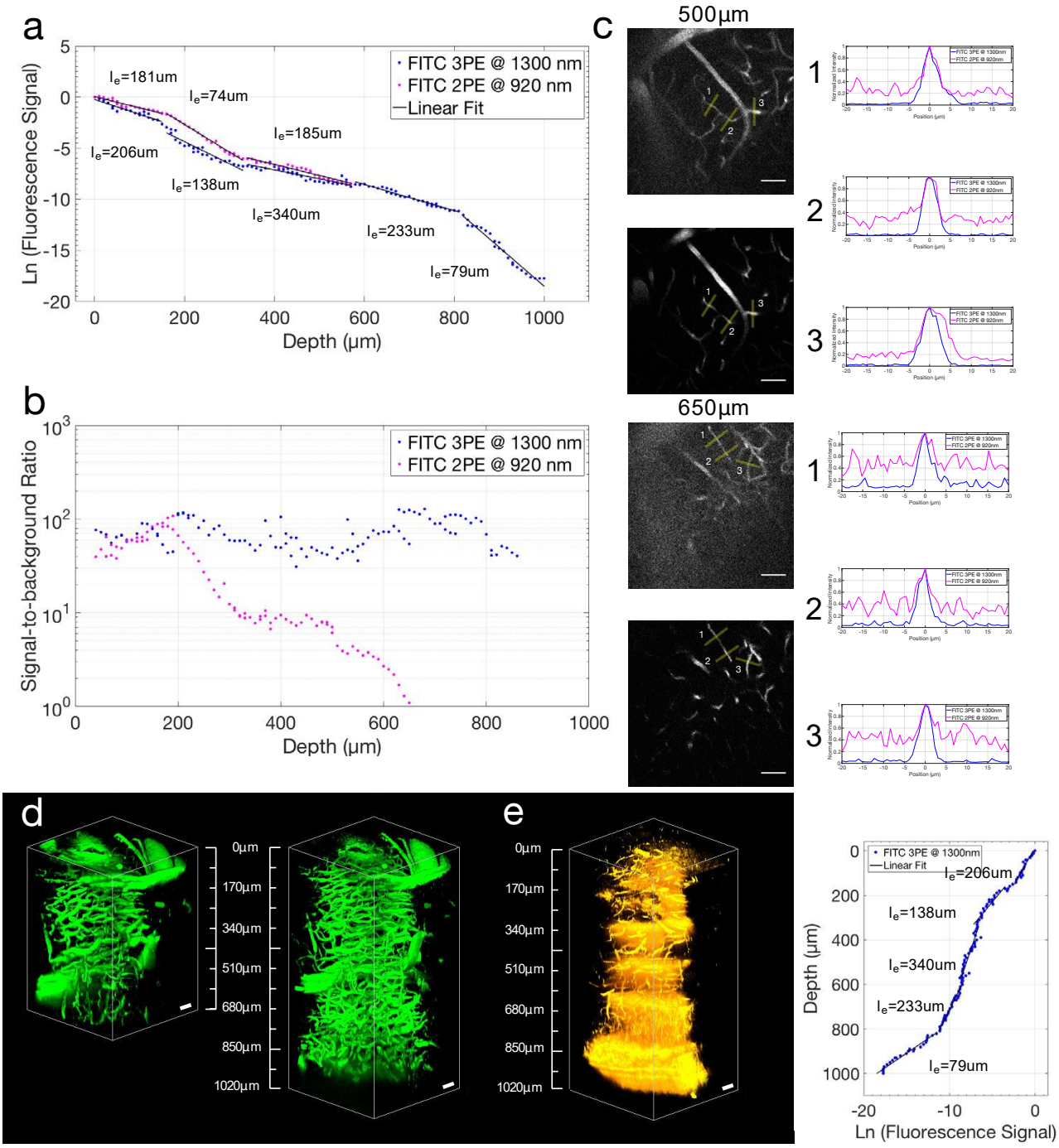

Figure 1. Comparison of fluorescein (FITC)-labeled blood vessels imaged by 2PM with 920 nm excitation and 3PM with 1300 nm excitation. a, Signal decay curve for 2PM and 3PM. Signal is normalized to the square or cubic of power for 2PM or 3PM, respectively, and both curves are normalized to their maximum at the surface. Effective attenuation lengths (l_e) are labeled next to the curves. b. SBR comparison at different depths for 2PM and 3PM. c. 2PM (top) and 3PM (bottom) images of fluorescein-labeled blood vessels at 500 μm and 650 μm. The two images were displayed with the same contrast settings (top 0.3% saturation). Scale bar, 50 μm. SBR measurements along the line profiles across different blood vessels (yellow lines) are shown on the right. d. 3D reconstruction of 2PM (left) and 3PM (right), depth is labeled in the middle. Scale bar, 50 μm. e. Left, 3D reconstruction of THG images from the cerebellum, depth is labeled on the left. Right, rotated signal decay curve from (a) to illustrate the corresponding relationship between fiber distribution and signal decay slope. Scale bar, 50 μm.

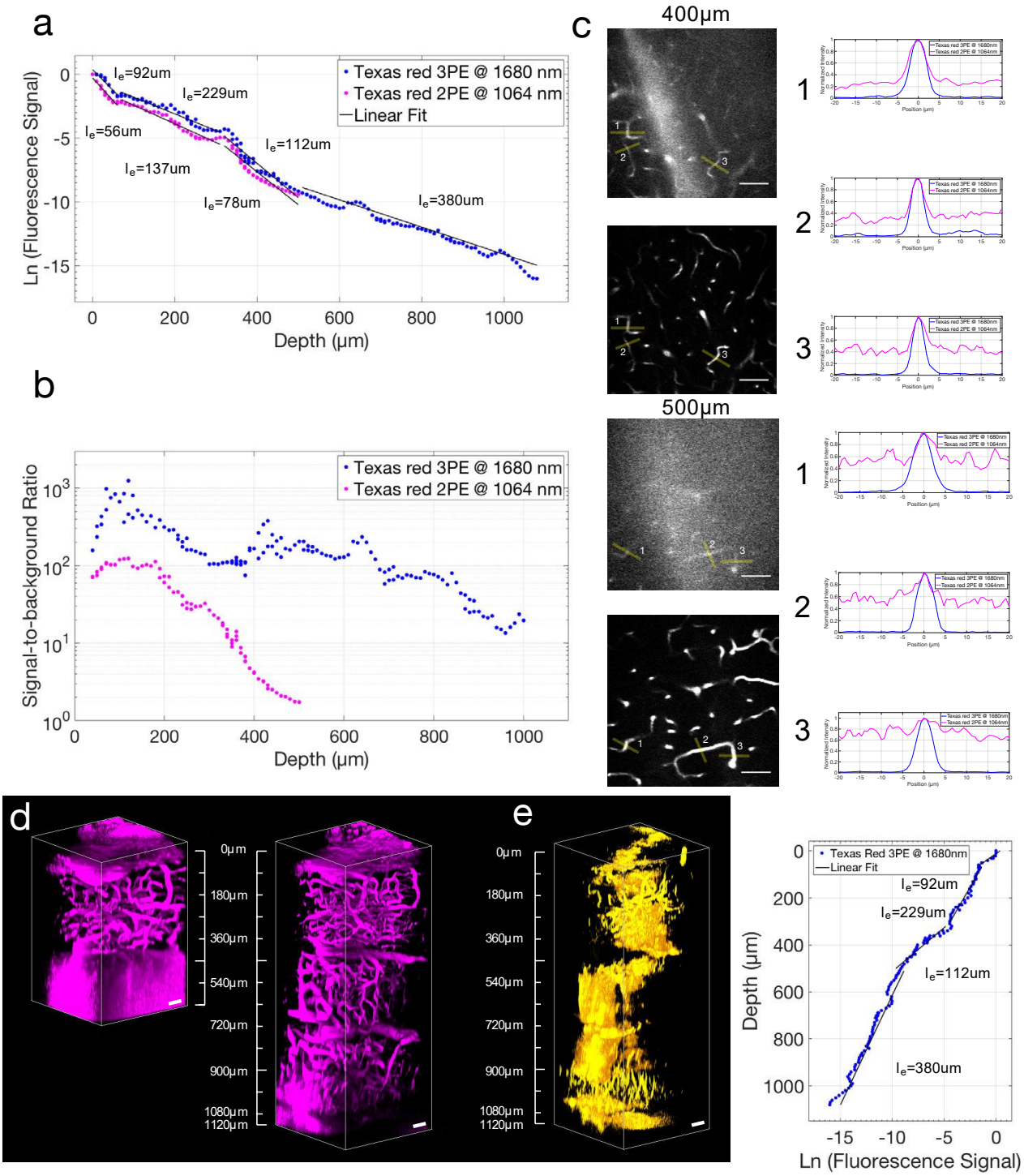

Figure 2. Comparison of Texas Red-labeled blood vessels imaged by 2PM with 1064 nm excitation and 3PM with 1680 nm excitation. a, Signal decay curve for 2PM and 3PM. Signal is normalized to the square or cubic of power for 2PM or 3PM,

respectively, both curves are normalized to their maximum at the surface. Effective attenuation lengths are labeled next to the curves. b. SBR comparison at different depths for 2PM and 3PM. c. 2PM (top) and 3PM (bottom) images of Texas Red-labeled blood vessels at 400 μm and 500 μm. The two images were displayed with the same contrast settings (top 0.3% saturation). Scale bar, 50 μm. SBR measurements along the line profiles across different blood vessels (yellow lines) are shown on the right. d. 3D reconstruction of 2PM (left) and 3PM (right) images, depth is labeled in the middle. Scale bar, 50 μm. e. Left, 3D reconstruction of THG images from the cerebellum, depth is labeled on the left. Right, rotated signal decay curve from (a) to illustrate the corresponding relationship between fiber distribution and signal decay slope. Scale bar, 50 μm.

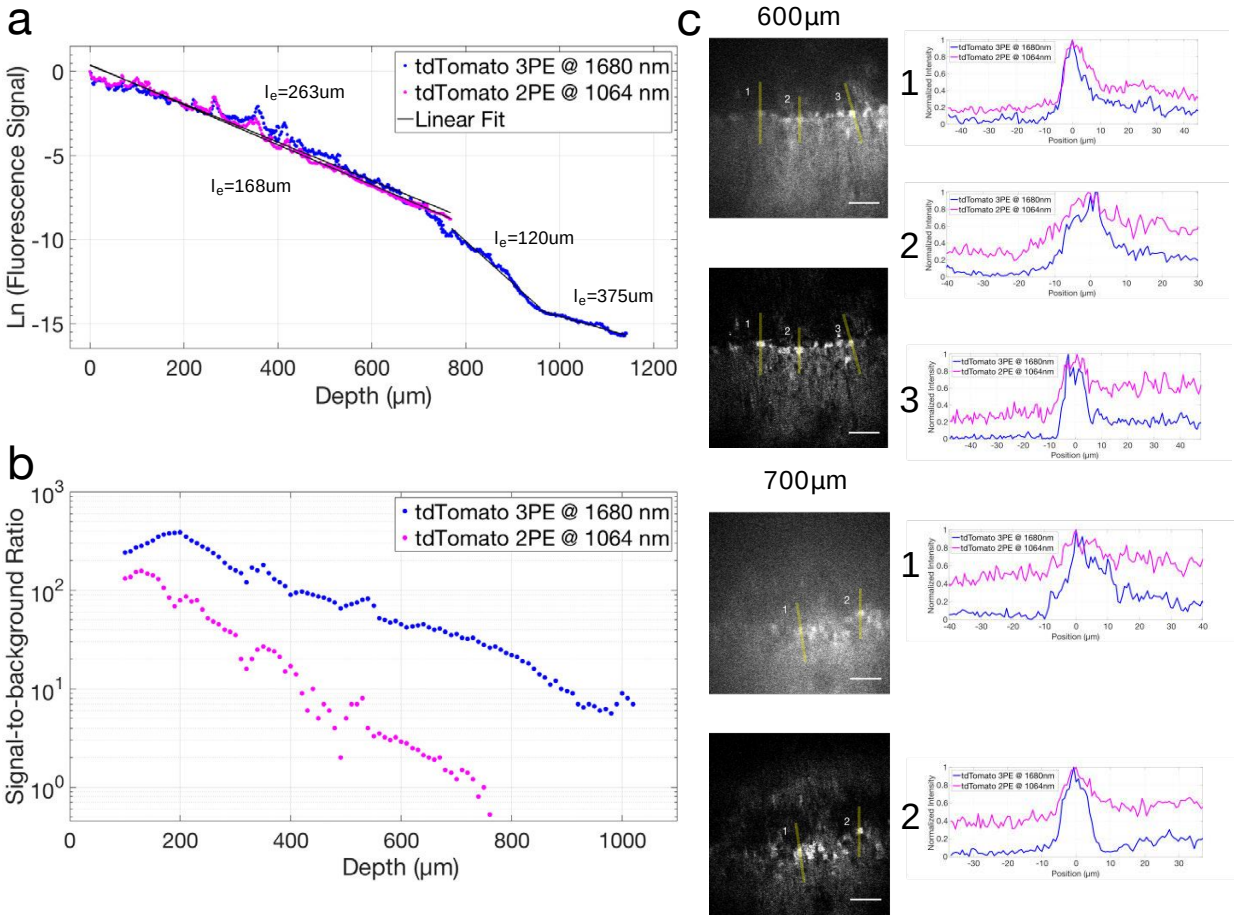

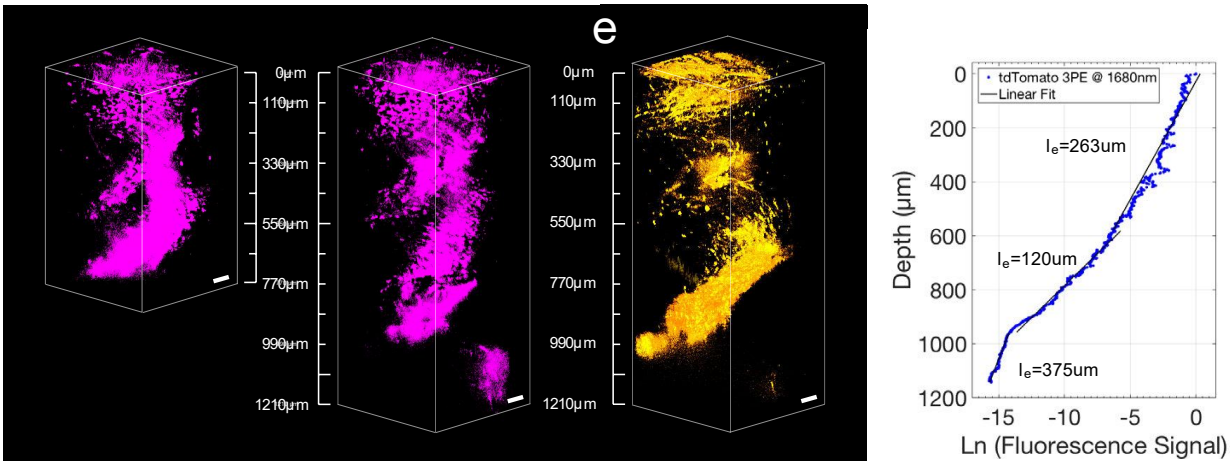

Figure 3. Comparison of tdTomato-labeled neurons imaged by 2PM with 1064 nm excitation and 3PM with 1680 nm excitation. a, Signal decay curve for 2PM and 3PM. Signal is normalized to the square or cubic of power for 2PM or 3PM, respectively, both curves are normalized to their maximum on the surface. Effective attenuation lengths are labeled next to the curves. b. SBR comparison at different depths for 2PM and 3PM. c. 2PM (top) and 3PM (bottom) images of fluorescein-labeled blood vessels at 600 μm and 700 μm. The two images were displayed with the same contrast settings (top 0.3% saturation). Scale bar, 50 μm. SBR measurements along the line profiles across different blood vessels (yellow lines) are shown on the right. d. 3D reconstruction of 2PM (left) and 3PM (right) images, depth is labeled in the middle. Scale bar, 50 μm. e. Left, 3D reconstruction of THG images from the cerebellum, depth is labeled on the left. Right, rotated signal decay curve from (a) to illustrate the corresponding relationship between fiber distribution and signal decay slope. Scale bar, 50 μm.

4. CONCLUSION

We demonstrate that 3PM can image deeper than 2PM for blood vessels as well as neurons in the same intact mouse cerebellum for both green and red fluorophores.

REFERENCES

[1] Theer, P., Hasan, M. T. and Denk, W., "Two-photon imaging to a depth of 1000 μm in living brains by use of a Ti:Al_2O_3 regenerative amplifier," Opt. Lett. **28**(12), 1022 (2003).

[2] Horton, N. G., Wang, K., Kobat, D., Clark, C. G., Wise, F. W., Schaffer, C. B. and Xu, C., "In vivo three-photon microscopy of subcortical structures within an intact mouse brain," Nat. Photonics **7**(3), 205–209 (2013).

[3] Ouzounov, D. G., Wang, T., Wang, M., Feng, D. D., Horton, N. G., Cruz-Hernández, J. C., Cheng, Y.-T., Reimer, J., Tolias, A. S., Nishimura, N. and Xu, C., "In vivo three-photon imaging of activity of GCaMP6-labeled neurons deep in intact mouse brain," Nat. Methods **14**(4), 388–390 (2017).

[4] Sullivan, M. R., Nimmerjahn, A., Sarkisov, D. V., Helmchen, F. and Wang, S. S.-H., "In vivo calcium imaging of circuit activity in cerebellar cortex," J. Neurophysiol. **94**(2), 1636–1644 (2005).

[5] Hoogland, T. M., Kuhn, B., Göbel, W., Huang, W., Nakai, J., Helmchen, F., Flint, J. and Wang, S. S.-H., "Radially expanding transglial calcium waves in the intact cerebellum," Proc. Natl. Acad. Sci. **106**(9), 3496–3501 (2009).